POAC'13
Espoo, Finland

Proceedings of the 22nd International Conference on
Port and Ocean Engineering under Arctic Conditions
June 9-13, 2013
Espoo, Finland

ICE PILING UP AND ICE LOADS ON NARROW STRUCTURES: LABORATORY EXPERIMENTS AND MODELLING OF KINEMATICS

Aleksey Marchenko[1], Dmitry Onishchenko[2]
[1]The University Centre in Svalbard, Longyearbyen, Norway
[2]Gazprom VNIIGAZ LLC, Russia

ABSTRACT
Kinematic model of the ice piling up near a fixed structure is formulated and steady pile solutions are analyzed for cylindrical structure of arbitrary shape. Conditions when the pile could be grounded are discussed. Experimental study of ice loads on vertical indenter pushed through the ice by hydraulic cylinder was performed in the ice tank in the UNIS cold laboratory. The indenter, which was equipped with an artificial bottom at the end for imitating shallow water effect, was pushed through the ice. The load on the piston was measured by a load cell with 50 Hz sampling frequency. Experiment was performed twice per day during several days in the same ice so that after several cycles the ice pile formed in the front on the indenter. Time records of the ice load versus the time are analysed and discussed in the paper.

1. INTRODUCTION
Study of ice interaction with relatively narrow structures in shallow water is important for offshore development in estuaries of northern rivers, e.g. in the Ob' Bay, the Kara sea. In such regions the ice is almost fresh. Its thickness can reach 1-2 meters depending on winter weather conditions. During winter season ice here doesn't have any regular drift, but can have displacements along the stream way caused by variations of water level due to tide, weather changes and spring water run-off.

Impact of the moving ice against fixed offshore structures is accompanied by ice piling up on structure walls. Ice piles can potentially extend to the water bottom and influence ice loads on structures and seabed (Karulin et al., 2007). Ice piling up near shoulder ice barriers and piles is considered as an ice protection for shallow water installations (Evers and Weihrauch, 2004; Barker and Timco, 2005; Gurtner et al., 2006). The ice piles are consolidated when displacements of ice cover are absent and the ice is in rest. Repeated displacements of consolidated ice piles can produce strong actions on offshore structures and cause their damage.

Effect of ice piling up on shoreline and sloping structures was described and analyzed theoretically in numerous papers (see e.g., Kovacs and Sodhi, 1980; Christinsen, 1994). Depending on structure size and ice floe size three different limitations are applicable for the engineering analysis: limiting driving force, limited ice strength and limited kinetic energy

(Croasdale, 1984). In case of ice piling up on a shore line or a wide sloping structure wind drag forces and ice pressure are main limiting factors for ice loads and ice pile sizes. In case of relatively narrow structures the main limiting factor is ice strength. Kinetic energy effect becomes more important for both wide and narrow structures with the increasing of the ice speed. 2D numerical simulations demonstrated the elongation of ice piles in horizontal direction after the pile sail height has reached critical value (Hopkins, 1994). Forces induced by ice piling up on shores and coastal structures were modelled using continuum mechanics approach based on 2D viscous rheology of ice rubble and mass balance equation taking into account variations of ice concentration and ice rubble thickness (Barker et al., 2001). 2D discrete element modelling of ice floating rubble loads on a sloping wall was performed as well (Paavilainen et al., 2011; 2013). Configurations of ice rubble piles constructed with discrete elements models show mean values of slope angles below 30^o degrees.

In case of ice interaction with a wall of finite width the effects of broken ice flow around the structure (clearing) and formation of rubble false bow influence the ice pile sizes and limit ice loads on the structure (Ettema and Nixon, 1998). Simple analysis of the mass balance equation describing kinematics of ice rubble around a wall demonstrates the existence of a steady pile solution when the ice outflux due to the clearing is in a balance with the ice influx into the rubble (Marchenko, 2010). This approach is similar to the consideration of crushed ice balance in narrow contact zones (Jordaan et al., 1988). In the present paper we develop further the analysis of the mass balance equation to estimate the sizes of steady ice piles near a fixed structure with relatively steep walls assuming that ice crushing presents main mechanism of the ice destruction near the structure. The second part of the paper based on new experimental results is related to the investigation of the ice loads on a fixed structure created by consolidated rubble ice pile which was formed around the structure earlier. Two parts of the paper are not related to each other as theory and experiment. The considerations and statement of the problems formulated in the paper are appeared to be relevant for the planned installations in the Ob' Bay of the Kara Sea.

2. KINEMATICS OF ICE PILING UP NEAR A FIXED STRUCTURE

A pile of broken ice is formed around fixed structure when level ice drifts against the structure (Fig. 1). Broken ice also drifts around the structure together with drifting level ice. It is assumed that hydrostatic equilibrium is not established in the ice pile when the ice is thick. The mass balance equation for the broken ice in the sail or the keel of the pile is written as follows (Marchenko, 2006, 2010)

$$\frac{\partial U_p}{\partial t} + \frac{\partial (v_\tau U_p)}{\partial s} = \frac{\kappa (\mathbf{v}_i \cdot \mathbf{n}) h_i}{1 - p}, \qquad (1)$$

where U_p is the area of vertical cross-section of the sail or keel in perpendicular direction to the structure wall, s is the length of the line L formed by the cross-section of the water surface and the structure wall, t is the time, $\mathbf{n}$ is the unit normal vector to the line L in the horizontal plane, v_τ is the tangential to the wall velocity of broken ice, p is the macroscopic porosity of the ice pile, h_i is the level ice thickness, and $\mathbf{v}_i$ is the level ice velocity. Coefficient κ shows the redistribution of broken ice between the sail and the keel. One has

$\kappa = 0.5$ when the same amounts of broken ice feed the sail and the keel. When the keel is grounded on shallow water and all flow of broken ice enters the sail only the coefficient κ is equal to 1.

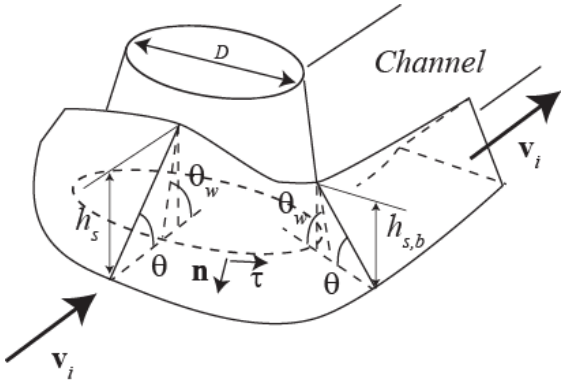

Figure 1. Scheme of the ice pile formation near the fixed structure.

Integrating equation (1) along the line L and assuming that the tangential velocity of broken ice v_τ is equal to the level ice velocity $v_i = |\mathbf{v}_i|$ at the sides of the structure we find

$$\frac{d}{dt}\int_{s_-}^{s_+} U_p ds + (U_{p,+} + U_{p,-})v_i = \frac{\kappa v_i h_i D}{1-p}, \tag{2}$$

where D is the structure width in the direction perpendicular to the ice drift, $U_{p,+}$ and $U_{p,-}$ are the areas of vertical cross-sections of the sail and the keel, respectively, at the edges of the structure. Two terms in the left part of equation (2) are positive. The second term increases with the time when the pile growing up. The right part of equation (2) is a constant when the velocity of ice drift v_i is constant. Therefore the first term in the left part of equation (2) tends to zero, and the pile tends to a steady state with the time.

Equation (2) shows that steady ice pile satisfies the condition

$$U_{p,+} + U_{p,-} = \frac{\kappa h_i D}{1-p}. \tag{3}$$

Consider an ice pile symmetric with respect to the vertical plane parallel to the direction of the level ice drift and assume that the surface of the ice pile coincides with a plane inclined under angle θ to the horizontal plane. The areas of vertical cross-sections of the sail and the keel at the edges of the structure are expressed by the formula

$$U_{s,+} = U_{s,-} = \frac{h_{s,b}^2}{2}\left(\frac{1}{\tan\theta} - \frac{1}{\tan\theta_w}\right),\ U_{k,+} = U_{k,-} = \frac{h_{k,b}^2}{2}\left(\frac{1}{\tan\theta} + \frac{1}{\tan\theta_w}\right), \tag{4}$$

where θ_w is the angle between the structure wall and the horizontal plane, $h_{s,b}$ and $h_{k,b}$ are the sail height and the keel draft near the structure edges (Fig. 1).

The sail height and the keel draft near the structure edges are found after the substitution of formula (4) into formula (3) as follows

$$h_{s,b} = \sqrt{\frac{2\kappa h_i D \tan\theta \tan\theta_w}{(1-p)(\tan\theta_w - \tan\theta)}}\,,\; h_{k,b} = \sqrt{\frac{2\kappa h_i D \tan\theta \tan\theta_w}{(1-p)(\tan\theta_w + \tan\theta)}}\,. \qquad (5)$$

The shape of the sail height and the keel draft of a steady pile near the structure is calculated from equation (1) in stationary form

$$\frac{d(v_\tau h_s^2)}{ds} = \kappa \frac{(\mathbf{v}_i \cdot \mathbf{n}) h_i}{1-p} \frac{\tan\theta \tan\theta_w}{\tan\theta_w - \tan\theta}\,,\; \frac{d(v_\tau h_k^2)}{ds} = \kappa \frac{(\mathbf{v}_i \cdot \mathbf{n}) h_i}{1-p} \frac{\tan\theta \tan\theta_w}{\tan\theta_w + \tan\theta}\,. \qquad (6)$$

Solution of differential equation (6) in the range $s \in (-s_b/2, s_b/2)$ with boundary conditions (5) is written as

$$\gamma h_s^2 = h_{s,b}^2 - \frac{\kappa h_i}{1-p} \frac{\tan\theta \tan\theta_w}{\tan\theta_w - \tan\theta} \int_{s_b/2}^{s} (\mathbf{i} \cdot \mathbf{n}) ds\,,\; \gamma h_k^2 = h_{k,b}^2 - \frac{\kappa h_i}{1-p} \frac{\tan\theta \tan\theta_w}{\tan\theta_w + \tan\theta} \int_{s_b/2}^{s} (\mathbf{i} \cdot \mathbf{n}) ds$$

$$\gamma = \frac{v_\tau}{v_i}\,,\; \mathbf{i} = \mathbf{v}_i / v_i\,. \qquad (7)$$

On the wall inclined to the direction of the ice drift we have that $v_\tau = (\mathbf{v}_i \cdot \boldsymbol{\tau})$, where $\boldsymbol{\tau}$ is the unit tangential vector to the structure wall in the horizontal plane. Parameter γ tends to zero when the angle between the ice drift direction and vector $\boldsymbol{\tau}$ tends to 90^o, and $h_{s,k} \to \infty$. In reality this singularity is not realised because of the formation of adjoined ice wedge taking a role of a structure wall. Criterion for the formation of adjoined ice wedge could be formulated in the form

$$\frac{dh_p}{ds} = \tan\theta\,. \qquad (8)$$

Condition (8) sets up that slope angle of the pile along the structure wall should not exceed the slope angle θ.

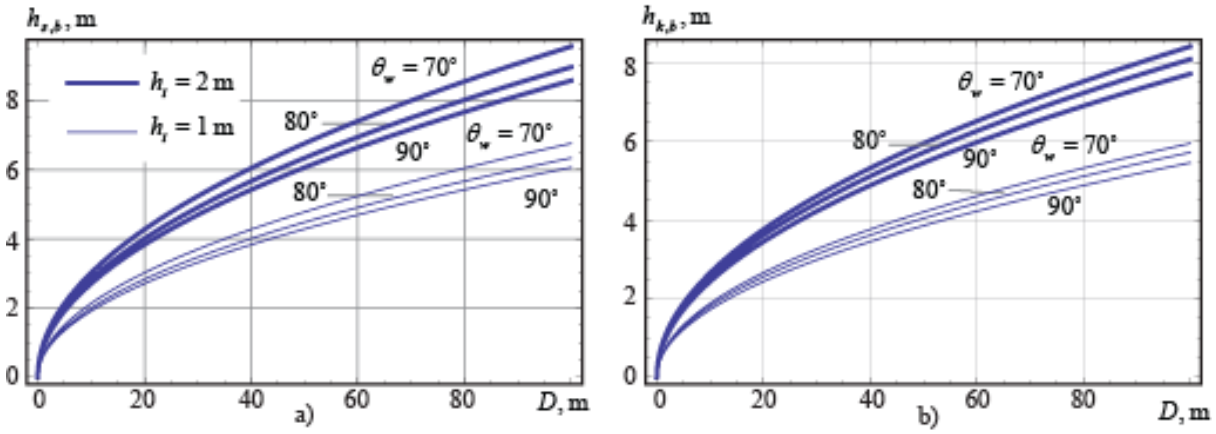

Figure 2. Sail height (a) and keel draft (b) of steady ice piles versus the structure width.

The sail heights $h_{s,b}$ and keel drafts $h_{k,b}$ calculated with formula (5) are shown in Fig. 2 versus the structure width D with $\kappa = 0.5$ and two values of the level ice thickness $h_i = 1\,\text{m}$

and $h_i = 2\,\text{m}$. Slope angle of the structure wall θ_w and level ice thickness are shown in the figure. It is assumed that $\theta = 30^\circ$ and $p = 0.2$. One can see that the keel draft $h_{k,b}$ doesn't exceed 4 m when the structure width is less than 20 m. The keel draft doesn't exceed 9 m for wide structures. The values of $h_{s,b}$ and $h_{k,b}$ calculated with $h_i = 2\,\text{m}$ shows also the sail height of steady piles with grounded keel when the thickness of level ice is 1m.

3. DESCRIPTION OF LABORATORY EXPERIMENTS

Experiments were performed in the ice tank of the University Centre in Svalbard. The sizes of the ice tank are 1.5m x 1m x 0.7m (Fig. 3). The walls and the bottom of the tank are equipped by a heating system supporting their temperature at the freezing point of the water inside the tank. It provides ice growth from the water surface in downward direction in the tank. The tank was filled by a mixture of sea water from the fjord with salinity 34 ppt and fresh water. Altogether together three sets of experiments were performed to measure ice force on the indenter pushed through the level ice with an ice pile in the front of the indenter. The room temperature was set to -15°C in the first set and to -20°C in the second and third sets of experiments. Actual ice temperature near the indenter was not measured.

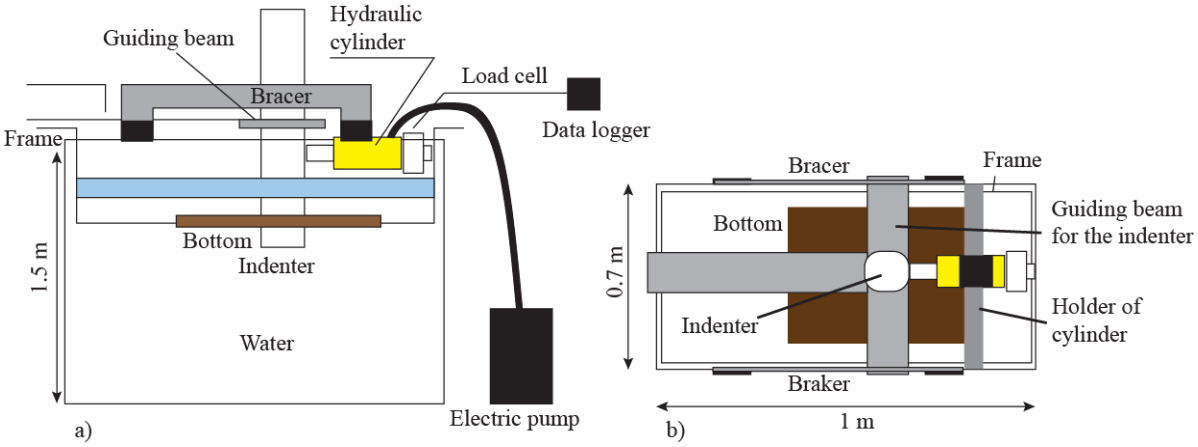

Figure 3. Scheme of the indentation test in the ice tank: side view (a) and in-plane view (b).

The scheme of experiments is performed in Fig. 3a and Fig. 3b in the vertical and horizontal planes respectively. The tank walls were protected from compressive loads by a metal frame mounted on the tank. Metal guiding beams of the cross shape were welded to the vertical indenter of square shape (6x6cm) in the horizontal cross-section. The photograph of the indenter with guiding beams is shown in Fig. 4a. Horizontal or inclined bottom was mounted on the end of the indenter so that a distance from the water surface to the horizontal bottom was equal to 10 cm in the first set of experiments and 12 cm in the second set of experiments. The third set of experiments was performed when the bottom slope to the horizontal plane was equal 20°. Vertical displacements of the guiding beams were limited by two bracers allowing the sliding of the cross in horizontal directions only. Hydraulic cylinder with a maximal load 10 T and 15 cm stroke was fixed in the horizontal position by a pipe holder. Load cell was mounted between the indenter and the metal frame. The cylinder and the load cell are shown in Fig. 4b. Sampling frequency of the load cell was 100 Hz. The displacement rate of the piston of the hydraulic cylinder was 3 mm/s in the first set of experiments and 3.5 mm/s in the second and the third sets of experiments.

The first and the second set of experiments included five stages. In the first stage the indenter moved against the level ice on the distance about 15 cm. Then the indenter was returned back

to the initial position, and all broken ice pieces were placed in the front of the indenter to imitate an ice pile. The second stage of the experiment was performed after several hours when the ice in the channel and the pile were frozen. The procedure repeated four times. Each day two experiment were performed in the morning and afternoon with the time interval between them about 5 hours. Time interval between the afternoon and the next morning experiments was about 20 hours. The third set of experiments with inclined bottom included only 2 stages with time interval between them 20 hours.

a) b)

Figure 4. Indenter with inclined and horizontal bottoms and guiding beams (a). Load cell and hydraulic cylinder in the holder inside the ice tank (b).

4. RESULTS OF EXPERIMENTAL STUDIES

Results of the first and the second sets of experiments are shown in Fig. 5 and in Tables 1, 2. The ice was destroyed by a crushing when indenter moved against the level ice of 1 cm thickness. The loads dropped with random periodicity when relatively large ice fragments were separated and flip over in the front or from the sides of the indenter (Fig 5a). The duration of such events was 3-5 seconds. The first peak loads was observed in the both experiments. Therewith variations of ice load during the experiments were comparable or higher the first peak load.

The first peak loads are well recognized in Fig. 5b and Fig. 5d in all stages from 2 to 5 in the first and the second sets of experiments both. Therefore it was possible to introduce phases I and II of the experiments shown in Fig. 5b and Fig. 5d. In the phase I the ice load reaches maximum and brittle destruction of the ice pile sail is observed (Fig. 6). In the phase II the ice loads are smaller and distributed in the time more uniformly. Mean duration of the phase I is about 10 seconds, and mean duration of the phase II is about 50 seconds (Tables 1 and 2).

Ice pressure p was calculated with the formula $p = F/(h_i h_{ind})$, where F is measured load, h_i is level ice thickness, and $h_{ind} = 6\,\text{cm}$ is the size of the indenter. In the first set of experiments maximal pressure 3.92 MPa was reached on the last stage 5e (Table 1). In the second set of experiments maximal pressure 5.83 MPa was reached on the first stage 1m, although the pressure on stage 4m was also high 5.21 MPa (Table 2). Fluctuations of the ice load with frequency about 10 Hz were registered in all experiments (see, e.g., Fig. 5c). Fluctuations were absent when the load was small. Since the frequency was the same in all experiments the effect is probably related to the excitation of natural frequency of the rig under the influence of ice load.

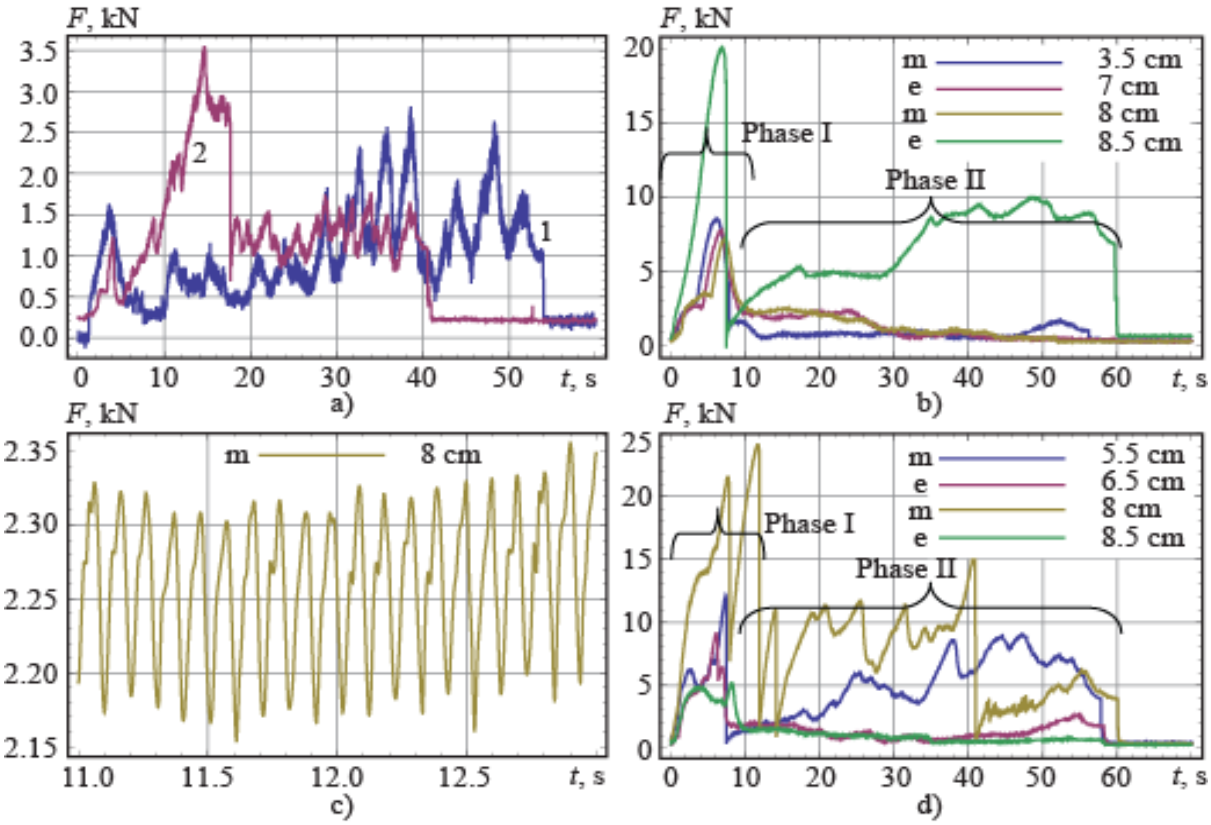

Figure 5. Ice load versus the time in the experiments 1e (the first set, curve 1) and 1m (the second set, curve 2) (a), 2m-5e (the first set) (b) and 2m-5e (the second set) (d). Example of vibrations of the load in the experiment 4m (the first set) (c).

The third set of experiments with inclined bottom included only 2 stages with time interval between them 20 hours. In the first stage the indenter with inclined bottom moved against level ice with thickness 2cm and salinity 1 ppt (Fig. 7a). Graph of ice load in Fig. 9a shows three local maxima. The first maximum seconds corresponds to the bending destruction of the ice due to the interaction with inclined bottom. The interaction was accompanied by brittle formation of three radial cracks and one circumferential crack. The load increased to maximal value and dropped to almost zero in 2 seconds. The third highest maximum of the load corresponds to the ice crashing due to the interaction with the indenter behind of the inclined bottom. Fluctuations of the ice load with frequency about 10 Hz are shown in Fig. 9c.

a) b)

Figure 6. Indenter and ice before (a) and after (b) the experiment 4m in the second set of experiments.

Table 1. Results of the first set of experiments

	1e	2m	3e	4m	5e
Ice thickness, cm	1	3.5	7	8	8.5
Ice salinity, ppt	0.5	0.8	0.4	0.3	0.5
Maximal load Phase I, kN	0.7	8.5	8	7.2	20
Maximal pressure Phase I, MPa	1.16	4.04	1.90	1.50	3.92
Duration of Phase I, s	53	8	11	10	8
Maximal load Phase II, kN	0	1.7	2.3	2.4	10
Maximal pressure Phase II, MPa	0	0.81	0.54	0.50	1.961
Duration of Phase II, s	0	50	50	40	54

Table 2. Results of the second set of experiments

	1m	2m	3e	4m	5e
Ice thickness, cm	1	5.5	6.5	8	8.5
Ice salinity, ppt	1.24	1.66	3.26	2.04	2.14
Maximal load Phase I, kN	3.5	12	9	25	6
Maximal pressure Phase I, MPa	5.83	3.63	2.3	5.21	1.18
Duration of Phase I, s	40	8	8	12	10
Maximal load Phase II, kN	0	8.7	2.6	16	1.5
Maximal pressure Phase II, MPa	0	2.64	0.66	3.33	0.29
Duration of Phase II, s	0	52	50	50	50

After the first stage all broken ice pieces were placed in the water on the bottom slope for the imitation of grounded ice ridge in shallow water (Fig. 8a). The level ice thickness reached 6 cm after 20 hours and the second stage of the experiment was performed. The ice is lifted up along the bottom slope and then was cut by the indenter (Fig. 8b). Ice load versus the time is shown in Fig. 9b. The first peak load is related to the formation of circumferential crack due to the interaction of the ice with bottom slope. The load drops to the half of maximal value in 10 seconds, and then varies around this value during 50 seconds. The ice interaction with the indenter can be characterized as brittle crashing with formation of large amount of small ice pieces. Fluctuations of the ice load with frequency about 10 Hz are shown in Fig. 9d.

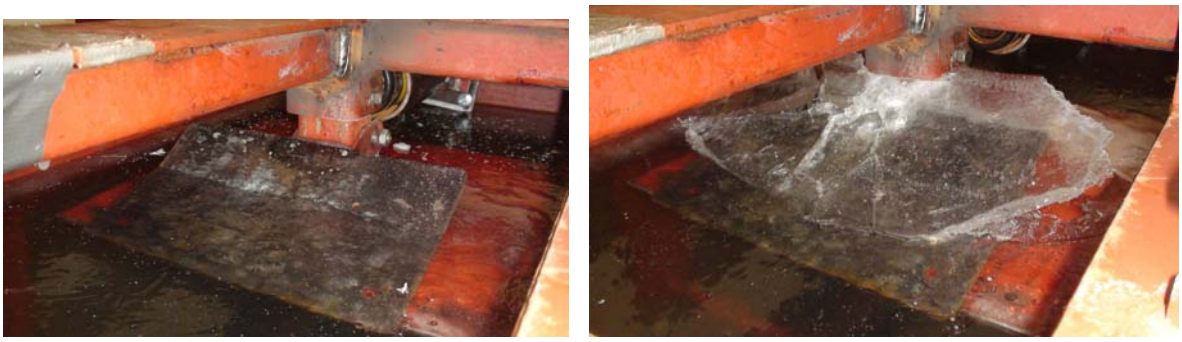

a) b)

Figure 7. Indenter and ice before (a) and after (b) the experiment 1 of the third set.

a) b)

Figure 8. Indenter and ice before (a) and after (b) the experiment 2 of the third set.

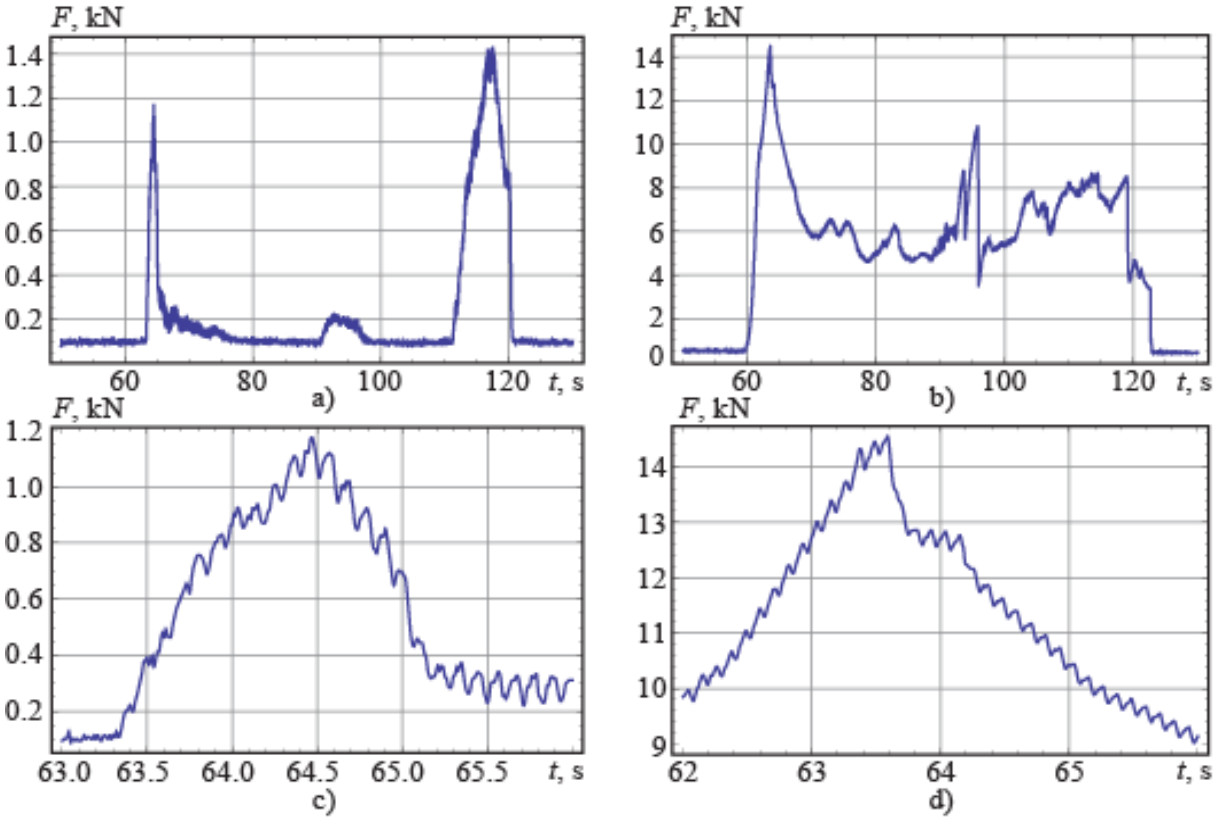

Figure 9. Ice load versus the time in the experiments 1 (a) and 2 (b) of the third set. Examples of vibrations of the load in the experiments 1 (c) and 2 (d).

4. CONCLUSIONS

Kinematic model of ice piling up near a structure based on the low of mass balance of broken ice in the pile and assumption about the slope angle of the pile is formulated. It is shown that the pile approaches to a steady state when the ice drifts against the structure with constant speed. Numerical estimates show that steady ice pile near a structure with diameter less than 20 m can be grounded when the water depth near the structure is smaller than 4 meters. Steady pile near a structure with diameter less than 40 m can be grounded when the water depth near the structure is smaller than 6 meters.

The experiments in the ice tank demonstrated that the interaction of the indenter with frozen ice pile consists of two phases. In the first phase brittle destruction of the pile keel is observed due to low air temperature. In the second phase the indenter penetrates through the keel.

Maximal loads are observed in the first phase. The duration of the first phase was about 10 seconds, and duration of the second phase was about 50 seconds in all experiments. Maximal loads increase with the increase of the pile dimensions. The influence of ice thickness and low air temperature on maximal loads is stronger than the influence of the bottom.

Ice interaction with inclined bottom near the indenter is accompanied by the formation of several radial cracks and one circumferential crack. The first peak load corresponds to the crack formation. The second peak load corresponds to brittle crashing of the cold ice due to the interaction with the indenter. Ice loads on the indenter were of the same order as in the experiments with the horizontal bottom. Fluctuations of ice loads with the frequency about 10 Hz were observed in all experiments.

REFERENCES

Barker, A., Timco, G., 2005. Iice rubble generation for offshore production structures: Current practices overview. Technical Report CHC-TR-030.

Barker, A., Timco, G., Sayed, M., 2001. Three-dimensional numerical simulation of ice pileup evolution along shorelines. Canadian Coastal Conference, 167-180.

Christensen, F.T., 1994. Ice ride-up and pile-up on shores and coastal structures. J. Coastal Research, 10(3), 681-701.

Croasdale, K.R., 1984. The limited driving force approach to ice loads. Proceedings Offshore Technology Conference (OTC-84), Paper OTC4716, Houston, Texas, pp. 57-64.

Ettema, R., Nixon, W.A., 1998. Ice rubble impact with a moored platform. IIHR Limited Distribution Report No. 147, Iowa Institute of Hydraulic Research The University of Iowa Iowa City, Iowa 52242-1585.

Gurtner, A., Gudmestad, O.T., Tørum, A., Løset, S., 2006. Innovative ice protection for shallow water drilling – Part I: Presentation of the concept. Proc. of the 25th Int. Conf. on Offshore Mechanics and Arctic Engineering, Hamburg, Germany.

Jordaan, I.J., Maes, M., Nadreau, J .P., 1988. The Crushing and Clearing of Ice in Fast Spherical Indentation Tests, OMAE '88, Proceedings of the Seventh International Offshore Mechanics and Arctic Engineering Symposium, Vol. 4, New York, American Society of Mechanical Engineers, 111-116.

Evers, K. and Weihrauch, A. (2004) Design and model testing of ice barriers for protection of offshore structures in shallow waters during winter. Proceedings of the 17th International Symposium on Ice, International Association of Hydraulic Engineering and Research (IAHR'04) Vol. 2, pp.124-131, St. Petersburg, CIS.

Karulin, E.B., Karulina, M.M., and Blagovidov, L.B., 2007. Ice modell tests on caisson platform in shallow water. Int. J. of Offshore and Polar Engineering, 17(4), 270-275.

Kovacs, A., Sodhi, D.S., 1980. Shore ice pile-up and ride-up: Field observations, models, theoretical analyses. Cold Regions Science and Technology, 2, 209288.

Marchenko, A.V., 2006. Method of calculation of ice loads by ice piling up on the wall. J. Applied Mathematics and Mechanics (PMM), 70, 387-398.

Marchenko, A.V., 2010. Modelling of ice piling up near offshore structures. Proc. of the 20th IAHR Symposium on Ice, Lahti, Finland, CD paper 014, 13 pp.

Paavilainen, J., Tuhkuri, J., Polojarvi, 2101. 2D numerical simulations of ice rubble formation process against an inclined structure. Cold Regions Science and Technology, 68, 20-34.

Paavilainen, J., Tuhkuri, J., 2103. Pressure distributions and force chains during simulated ice rubbling against sloping structures. Cold Regions Science and Technology, 85, 157-174.